Organic & Biomolecular Chemistry

PAPER

View Article Online
View Journal

Cite this: DOI: 10.1039/c6ob00177g

Selective recognition of *c-MYC* G-quadruplex DNA using prolinamide derivatives†

Ajay Chauhan,‡[a] Sushovan Paladhi,‡[a,b] Manish Debnath‡[b] and Jyotirmayee Dash*[a,b]

Received 21st January 2016,
Accepted 3rd March 2016

DOI: 10.1039/c6ob00177g

www.rsc.org/obc

Herein we report the design, synthesis, biophysical and biological evaluation of triazole containing prolinamide derivatives as selective *c-MYC* G-quadruplex binding ligands. A modular synthetic route has been devised for prolinamide derivatives using a copper(I) catalyzed azide–alkyne cycloaddition (CuAAC). The Förster resonance energy transfer (FRET) melting assay indicates that prolinamide trimers can significantly stabilize G-quadruplex structures over duplex DNA compared to prolinamide dimers. The fluorescent intercalator displacement (FID) assay shows that a trimer with prolinamide side chains at the *para*-position of the benzene ring can discriminate between different quadruplex structures and exhibits the highest binding affinity towards the *c-MYC* G-quadruplex structure. Molecular modeling studies reveal that the prolinamide trimer stacks upon the terminal G-quartet of the *c-MYC* G-quadruplex. Atomic force microscopy (AFM) analysis reveals that the tris-prolinamide ligand can be used to regulate the assembly of novel supramolecular nanoarchitectures. Further, *in vitro* cellular studies with human hepatocellular carcinoma (HepG2) cells indicate that the tris-prolinamide derivatives can inhibit cell proliferation and reduce *c-MYC* expression in cancer cells.

Introduction

G-quadruplexes are four-stranded DNA secondary structures formed by self-assembly of guanine rich single stranded DNA sequences.[1,2] One important G-quadruplex forming sequence is found in the nuclease hypersensitive element (NHE) III1, present in the P1 promoter of the *c-MYC* oncogene.[3] The *c-MYC* oncogene is associated with cell growth, proliferation and a range of malignant tumors.[4] Targeting the G-quadruplex found in the promoter region of the *c-MYC* gene is one of the few therapeutic opportunities that exist to gain control over the overexpression of the *c-MYC* protein.[5] It has been proposed that the transcription of the *c-MYC* oncogene can be substantially reduced by the formation and stabilization of G-quadruplex structures using small molecules.[5–7] Several classes of small molecules have been reported to bind and stabilize *c-MYC* G-quadruplex structures.[5,7,8] However, only a few ligands including porphyrins, quindolines, and carbazole derivatives[9–12] have been evaluated in the cellular system to exhibit potential anticancer activities.[12] Therefore, the development of new chemical scaffolds, which can selectively bind the *c-MYC* G-quadruplex, would provide a promising avenue in anticancer therapeutics. Furthermore, guanine-rich nucleic acid sequences have generated immense interest in the field nanotechnology due to their ability to form self-assembled higher-order nanostructures.[13]

Recently we have reported that prolinamide ligands can be designed for selectively interacting with quadruplex structures.[14] In the present study, we describe the design and synthesis of novel bis- and tris-prolinamide derivatives as potent G-quadruplex binding ligands. The tris-prolinamide derivatives with a 1,3,5-triphenylbenzene core can bind the *c-MYC* G-quadruplex and inhibit *c-MYC* expression *in vitro*. The AFM analysis reveals that a tris-prolinamide ligand can direct the assembly of the *c-MYC* G-quadruplex into chain like nanostructures.

Results and discussion

Design and synthesis of ligands

We have previously reported that a prolinamide dimer can selectively interact with a quadruplex structure and inhibit growth of cancer cells.[14] Proline motifs are present in numerous natural products and bioactive peptides. Moses *et al.* reported that C3-symmetric ligands can stabilize G-quadruplexes over duplex DNA.[15] In this work, we have synthesized a series of bis- and tris-prolinamide derivatives linked to the aro-

[a]*Department of Chemical Sciences, Indian Institute of Science Education and Research Kolkata, Mohanpur, 741 252, India*
[b]*Department of Organic Chemistry, Indian Association for the Cultivation of Science, Jadavpur, Kolkata-700032, India. E-mail: ocjd@iacs.res.in*

†Electronic supplementary information (ESI) available: Synthetic procedures, characterization data of compounds, ^{1}H NMR and ^{13}C NMR spectra. See DOI: 10.1039/c6ob00177g

‡These authors contributed equally to this work.

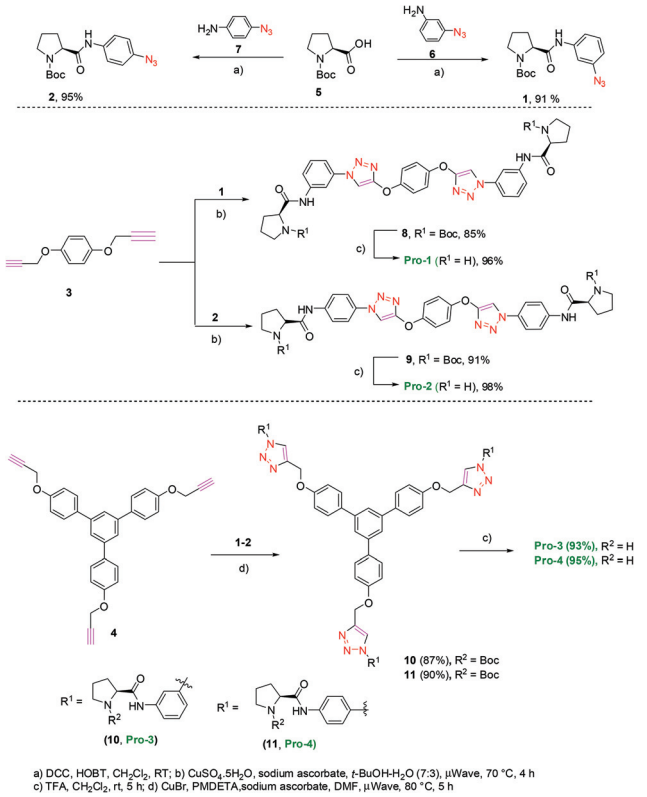

Scheme 1 Synthesis of prolinamide derivatives.

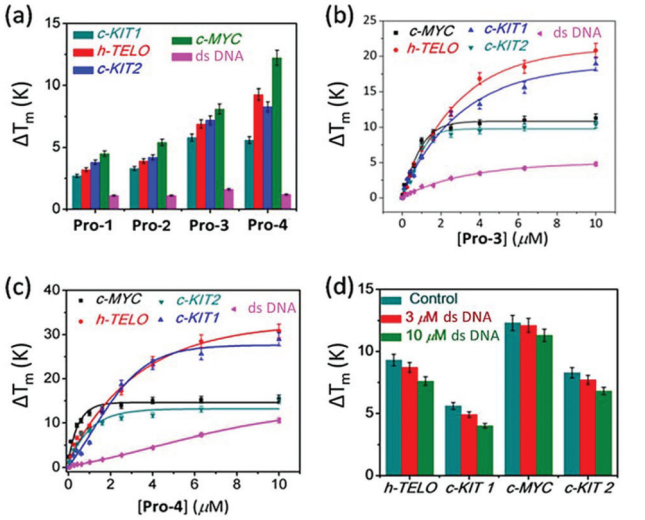

Fig. 1 (a) FRET stabilization potential of bis- and tris-prolinamide derivatives **Pro-1**, **Pro-2**, **Pro-3** and **Pro-4** (1.0 μM) upon binding to (*c-MYC*, *h-TELO*, *c-KIT1* and *c-KIT2*) quadruplexes and a ds-DNA; (b) thermal shift profiles for **Pro-3** upon stabilizing *c-MYC*, *h-TELO*, *c-KIT1* and *c-KIT2* quadruplexes and duplex DNA; buffer: 50 mM potassium cacodylate, pH 7.4. (c) Thermal shift profiles for **Pro-4** upon stabilizing *c-MYC*, *h-TELO*, *c-KIT1* and *c-KIT2* quadruplexes and ds-DNA; buffer: 50 mM potassium cacodylate, pH 7.4. (d) FRET competition assay of **Pro-4** (1.0 μM) for G-quadruplexes (200 nM) in the presence of duplex DNA (3.0 μM and 10.0 μM).

matic core. The resulting C2 and C3 symmetric bis- and tris-prolinamide derivatives **Pro-1** to **Pro-4** having a central aromatic core with prolinamide side chains could show selectivity for a particular quadruplex structure. The prolinamide ligands **Pro-1** to **Pro-4** were prepared using Cu(I) catalyzed azide–alkyne cycloaddition between azido-prolinamide derivatives **1** and **2** with di and tri-alkyne linkers **3** and **4** (Scheme 1).[14,16] The azido-prolinamides **1** and **2** were prepared in high isolated yields (91–95%) by amide coupling of *N*-Boc proline **5** with 3-azidoaniline **6** and 4-azidoaniline **7**, respectively. Subsequently, the azido-prolinamide derivatives **1** and **2** were linked with di-alkyne **3** using $CuSO_4{\cdot}5H_2O$ and sodium ascorbate in *t*-BuOH/H_2O (7 : 3) under microwave irradiation at 70 °C to yield the desired triazole linked bis-prolinamide derivatives **8** and **9** in excellent yields. The reaction of trialkyne **4** with azido-prolinamides **1** and **2** was then carried out using CuBr and PMDETA in DMF at 80 °C under microwave irradiation. The desired triazole containing tris-prolinamide derivatives **10** and **11** were obtained in high yields. The *N*-Boc deprotection was carried out using trifluoroacetic acid (TFA) in CH_2Cl_2 to afford the ligands **Pro-1** to **Pro-4** in 93–98% yields from the corresponding *N*-Boc prolinamide dimers **8**, **9** and trimers **10**, **11** (Scheme 1).

FRET melting assay

The stabilizing ability and selectivity of the ligands towards G-quadruplex DNA over duplex DNA was evaluated by the FRET melting assay,[17] which measures the changes in the melting temperature (ΔT_m) of the DNA in the presence of the ligands (Fig. 1). Four dual labeled (5′-FAM and 3′-TAMRA) G-quadruplex (*c-MYC*, *h-TELO*, *c-KIT1* and *c-KIT2*) forming sequences and a control duplex DNA were used in this study. As shown in Table 1, the tris-prolinamide derivatives **Pro-3** and **Pro-4** displayed significant selectivity towards G-quadruplexes compared to the ds DNA at 1 μM ligand concentration (Fig. 1b and c). Ligand **Pro-4** (1 μM) containing three *para*-prolinamide side chains exhibited the maximum stabilization towards *c-MYC* with a ΔT_m of ~12.3 K compared to ~9.3 K, ~5.6 K and ~8.4 K for *h-TELO*, *c-KIT1* and *c-KIT2* quadruplexes, respectively. In contrast, ligand **Pro-3** (1 μM) containing three *meta*-prolinamide side chains displayed moderate G-quadruplex stabilizing ability (Fig. 1b and c). However, ligands **Pro-1** and **Pro-2** containing two prolinamide side chains exhibited a comparatively weaker stabilizing ability and selectivity for all the investigated quadruplexes (Table 1).

The selectivity of ligand **Pro-4** for the G-quadruplexes over ds DNA was further evaluated using a competitive FRET-melting assay (Fig. 1d). The melting of the *c-MYC* G-quadruplex sequence with 1 μM **Pro-4** was performed in the presence of a ds-DNA competitor. As shown in Fig. 1d, only a small change in the stabilization for quadruplexes was observed even after addition of 10 μM ds DNA competitors (50 mol equivalent excess to the quadruplex). These results indicate that **Pro-4** shows selectivity for quadruplexes over ds DNA.

Table 1 G-quadruplex stabilisation potential (ΔT_m) measured by the FRET-melting assay[a,b]

DNA sequences	Pro-1	Pro-2	Pro-3	Pro-4
c-MYC	4.8 ± 0.4	5.2 ± 0.5	8.1 ± 0.7	12.3 ± 0.9
h-TELO	4.3 ± 0.3	4.5 ± 0.5	6.9 ± 0.5	9.3 ± 0.7
c-KIT1	4.1 ± 0.2	4.7 ± 0.4	5.8 ± 0.7	5.6 ± 0.8
c-KIT2	4.5 ± 0.3	4.4 ± 0.4	7.2 ± 0.8	8.4 ± 0.8
ds DNA	1.2 ± 0.1	1.3 ± 0.1	1.6 ± 0.2	1.2 ± 0.1

[a] T_m (°C) for *c-MYC* = (70 ± 1), *c-KIT1* = (53 ± 1), *c-KIT2* = (63 ± 1), *h-TELO* = (56 ± 1), ds DNA = (57 ± 1) in 60 mM potassium cacodylate buffer, pH 7.4 without ligands. [b] Errors were calculated as standard deviation of three independent experiments.

Collectively, these data suggested that tris-prolinamide derivatives **Pro-3** and **Pro-4** exhibit high stabilization potential for the quadruplexes in comparison with the bis-prolinamide derivatives. Further the melting shift profiles indicate that **Pro-4** shows the maximum stabilization potential for the *c-MYC* quadruplex in comparison with the other quadruplexes.

Fluorescence spectroscopy

The binding affinities of the tris-prolinamides **Pro-3** and **Pro-4** for the *c-MYC* G-quadruplex were determined using fluorescence spectroscopy (Fig. 2a, b and S1, ESI†).[18,19] The *c-MYC* quadruplex forming sequences end-labeled with 5′-FAM and 3′-FAM were titrated with the ligand **Pro-3** or **Pro-4** and the emission spectra were recorded. We have observed a decrease in the fluorescence emission of the attached fluorophores upon addition of the ligands to both the end-labeled G-quadruplexes. In agreement with the previous studies conducted for the ligand induced quenching of the fluorophore, the observed fluorescence quenching may be due to the binding of **Pro-3** or **Pro-4** to the quadruplexes in the proximity of the FAM in a non-radiative manner.[18] The binding association constant values corresponding to the binding of **Pro-3** and **Pro-4** to 5′-FAM labeled *c-MYC* were determined to be 1.7×10^5 M^{-1} and 2.8×10^5 M^{-1}, respectively. Compared to this, the association constant values due to the binding of **Pro-3** and **Pro-4** to 3′-FAM labeled *c-MYC* were 7.4×10^4 M^{-1} and 1.6×10^5 M^{-1}, respectively. The results indicate that the ligands **Pro-3** and **Pro-4** binds to the proximity of the 5′-end compared to the 3′-end of the G-quadruplex structure. These results also reveal that **Pro-4** binds to the *c-MYC* G-quadruplex with higher affinity than **Pro-3**. It is interesting to mention that no change in fluorescence intensity was observed upon addition of **Pro-3** or **Pro-4** to the FAM labeled duplex DNA (Fig. S1, ESI†). These results are in agreement with FRET melting analysis which shows that both the ligands show selectivity for the quadruplex structure over duplex DNA.

Next, the fluorescent intercalator displacement (FID) assay was employed to investigate the binding selectivity of **Pro-4** towards different G-quadruplexes.[20] This assay measures the decrease in fluorescence intensity upon the displacement of thiazole-orange (TO) from the G-quadruplex–TO complex by the ligand (Fig. 2c). The concentrations of the ligand **Pro-4**

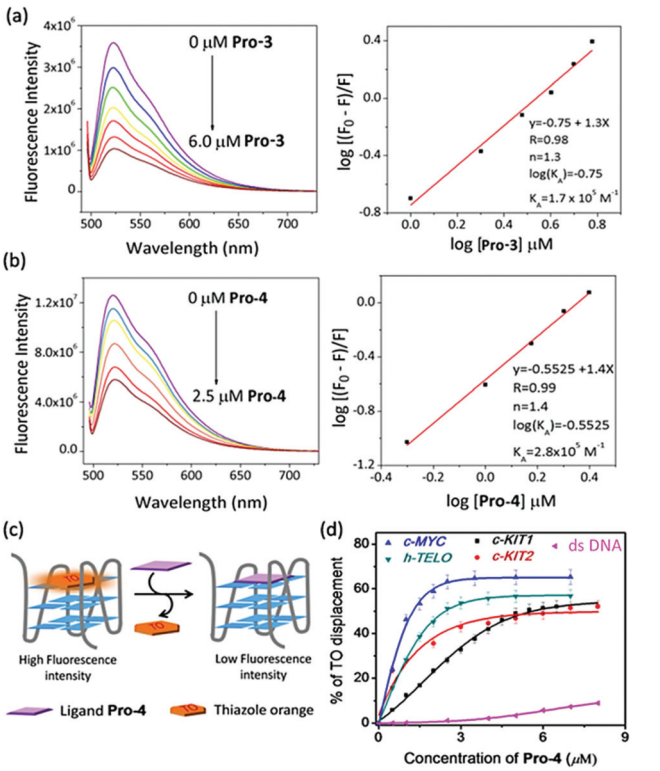

Fig. 2 (a) Fluorescence emission spectra of the 5′-FAM labeled *c-MYC* with increasing addition of **Pro-3** (Left). Plot of log[$(F_0 - F)/F$] as a function of log[**Pro-3**] (right); (b) fluorescence emission spectra of the 5′-FAM labeled *c-MYC* with increasing addition of **Pro-4** (Left). Plot of log[$(F_0 - F)/F$] as a function of log[**Pro-4**] (Right); (c) Schematic representation showing the principle of the TO displacement assay; (d) TO displacement by **Pro-4** from *c-KIT1*, *c-KIT2*, *c-MYC*, *h-TELO* G-quadruplexes and ds DNA; with increasing concentrations of **Pro-4** in buffer containing 100 mM KCl and 10 mM Tris·HCl, pH 7.4.

required to reduce the fluorescence intensity (TO) by 50% (DC_{50}) was determined for four G-quadruplexes (*c-MYC*, *c-KIT1*, *c-KIT2*, *h-TELO*) and a duplex DNA sequence (ds DNA). Ligand **Pro-4** displayed significant potency to displace TO from all the quadruplexes compared to ds DNA, indicating its selectivity towards the G-quadruplex DNA (Fig. 2d and Table 2). As shown in Table 2, **Pro-4** showed the highest affinity towards *c-MYC* with a DC_{50} value of 1.2 μM. However, higher concentrations

Table 2 DC_{50} obtained for ligand **Pro-4** from FID data[a]

DNA sequences	DC_{50} (μM)
c-MYC: 5′-(TGAG$_3$TG$_3$TAG$_3$TG$_3$TAA)-3′	1.2 ± 0.2
c-KIT1: 5′-(G$_3$AG$_3$CGCT G$_3$A G$_3$AG$_3$)-3′	5.5 ± 0.1
c-KIT2: 5′-(G$_3$CG$_3$CGCGA G$_3$AG$_4$)-3′	7.7 ± 0.4
h-TELO: 5′-(G$_3$TTAG$_3$TTAG$_3$TTAG$_3$)-3′	2.4 ± 0.1
ds DNA: 5′-CCAGTTCGTAGTAACCC-3′ 3′-GGTCAAGCATCATTGGG-5′	n.d.

[a] Errors were calculated as standard deviation of three independent experiments.

of **Pro-4** were required to displace 50% TO from *c-KIT1*, *c-KIT2* and *h-TELO* G-quadruplexes. The DC_{50} values of **Pro-4** were observed to be ~2.4 μM, ~5.5 μM and ~7.7 μM for *c-KIT1*, *c-KIT2* and *h-TELO* quadruplexes respectively. Therefore, **Pro-4** exhibits 2, 4.5 and 6 fold higher affinities towards *c-MYC* compared to *h-TELO*, *c-KIT1* and *c-KIT2* respectively. It is worth noting that ligand **Pro-4** could not even displace 50% TO from ds DNA at 10 μM ligand concentrations (Fig. 2d), indicating excellent selectivity of ligand **Pro-4** for quadruplexes over duplex DNA. These results are in agreement with the FRET melting data and indicate that **Pro-4** containing three *para*-prolinamide motifs and a 1,3,5-triphenylbenzene core displays superior selectivity for the G-quadruplex DNA over the duplex DNA, and exhibits significant stabilization for the *c-MYC* G-quadruplex.

AFM analysis

AFM has been widely used to visualize G-quadruplex based nanostructures[21] as well as G-quadruplex-ligand assembled nanostructures.[22] We have employed AFM to investigate the morphology of nanostructures obtained upon interaction of **Pro-4** with the *c-MYC* G-quadruplex (Fig. 3a and b). The AFM image of the *c-MYC* G-quadruplex (pre-folded with K^+) revealed a heterogeneous distribution of spherical particles with an average height of 2–4 nm (Fig. 3c, ESI†). Upon incubation of the *c-MYC* G-quadruplex with **Pro-4** resulted in the formation of linear and branched chain-like nanostructures. These chain-like structures have a mean length of 50–600 nm with an average height of 2–4 nm. The average height of the observed nanostructures (2–4 nm) of the *c-MYC* quadruplex in the presence and absence of the ligand **Pro-4** is close to the diameter of G-quartets (2.4 nm) as determined by X-ray crystallography. Therefore, it can be proposed that the discrete spherical structure of the *c-MYC* quadruplex is possibly observed due to the formation of individual G-quadruplexes in the presence of K^+ ions (Fig. 3c). In the presence of **Pro-4**, higher order surface aggregated structures of *c-MYC* quadruplexes are observed which may be attributed to the model proposed by Neidle and co-workers in which the two adjacent quadruplexes are stacked together and the quadruplex–quadruplex interface is stabilized by the **Pro-4** molecule.[23,24] Molecular modeling further suggested that **Pro-4** binds to *c-MYC* (PDB ID: 1XAV)[25] *via* end-stacking mode and stacks between two consecutive quadruplexes to form chain like structures. The modeling data indicate that ligand **Pro-4** undergoes conformational changes upon interacting with the *c-MYC* quadruplex. The planar aromatic region in **Pro-4** effectively stacks on the terminal G-quartet of the G-quadruplex DNA through π–π stacking and the prolinamide side chains interact with the groove and loop regions of the G-quadruplex (Fig. 3c and d). It allows conformational flexibility due to the presence of rotatable bonds unlike the rigid structure of many reported macrocyclic or planar heteroaromatic G-quadruplex binding ligands.[8,9,11,26] The best docking orientation of **Pro-4** with *c-MYC* showed an interaction energy value of −39.27 KJ mol^{-1}. In addition to this, circular dichroism (CD) spectroscopy suggested that binding of **Pro-4** does not distort the *c-MYC* parallel G-quadruplex conformation (Fig. S2, ESI†).

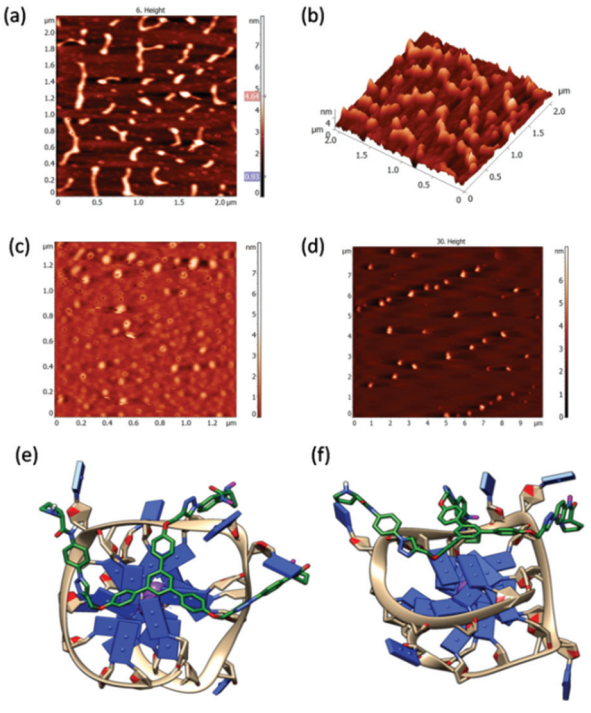

Fig. 3 (a) AFM 2D image for *c-MYC* (10 μM) in the presence of 10 μM **Pro-4** in aqueous buffer containing 100 mM KCl and 10 mM Tris·HCl at pH 7.4; (b) AFM 3D image for *c-MYC* (10 μM) in the presence of 10 μM **Pro-4** in aqueous buffer containing 100 mM KCl and 10 mM Tris·HCl at pH 7.4; AFM images of 10 μM *c-MYC* only (c) and 10 μM **Pro-4** only (d) in aqueous buffer containing 100 mM KCl and 10 mM Tris·HCl at pH 7.4; docked conformations of the **Pro-4** with *c-MYC* quadruplex (PDB ID: 1XAV), (e) top view and (f) side view.

Growth inhibition assay

The ability of the tris-prolinamide derivatives **Pro-3** and **Pro-4** to inhibit the growth of HepG2 cancer cells was investigated using the MTT assay.[27] The IC_{50} values for growth inhibition of HepG2 cells were found to be ~13.4 μM and ~7.1 μM for **Pro-3** and **Pro-4**, respectively (Fig. S3, ESI†). And both these ligands (**Pro-3** and **Pro-4**) didn't show any cytotoxicity towards a normal cell line (C2C12, mouse myoblast), even at 50 μM concentration.

Regulation of *c-MYC* expression

To evaluate the inhibitory abilities of **Pro-3** and **Pro-4** on the expression of *c-MYC* (Fig. 4a), qRT-PCR and western blot assays were carried out using HepG2 cells. HepG2 cells were treated with the IC_{50} dose (13.4 and 7.1 μM) of **Pro-3** and **Pro-4** for 24 h and then the total *c-MYC* RNA and protein levels were quantified relative to the expression of GAPDH as the housekeeping gene. Analysis of the qRT-PCR data revealed that **Pro-4** reduced the level of *c-MYC* RNA by 65 ± 5% relative to the control (Fig. 4b). Further, western blot analysis using the anti-

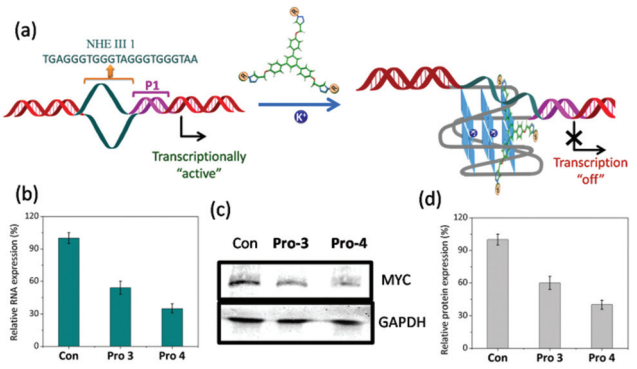

Fig. 4 Effect of **Pro-3** and **Pro-4** on the expression of the *c-MYC* protein in human cancer cells: (a) schematic representation of ligand induced transcriptional down-regulation of the *c-MYC* gene; (b) determination of transcriptional regulation of *c-MYC* RNA in the presence of an IC_{50} dose of **Pro-3** or **Pro-4** in cancer cells by qRT-PCR and quantified by the comparative threshold method using GAPDH as the housekeeping gene; (c) immunoreactive bands of the *MYC* protein were analyzed by western blotting; (d) densitometric analyses of immunoblots showing a reduced level of the *MYC* protein upon treatment with **Pro-3** and **Pro-4**. The results are representative of five independent experiments with two replicates. The data are shown as mean ± SD. $*P < 0.05$, $\#P < 0.01$, *versus* untreated cancer cells.

MYC antibody showed that the expression of the *MYC* protein was reduced by 60 ± 3% compared to the control (Fig. 4c). **Pro-3** exhibited a less pronounced effect on the *c-MYC* expression with 46 ± 4% and 40 ± 3% reduction in the RNA and protein levels relative to the control (Fig. 4b–d). However, upon treatment of the HepG2 cells with **Pro-3** or **Pro-4**, no significant changes in the GAPDH RNA or protein level were observed. These results indicate that both **Pro-3** and **Pro-4** can down-regulate the *c-MYC* expression in cancer cells but the more competent G-quadruplex binder **Pro-4** is more effective towards the down-regulation of *c-MYC* expression.

Conclusion

The interaction of new prolinamide derivatives with a variety of DNA sequences has been investigated. These studies demonstrate that prolinamide derivatives can selectively bind and stabilize G-quadruplex structures. Ligand **Pro-4** containing three *para*-prolinamide units is found to be the most promising *c-MYC* G-quadruplex binding ligand compared to other bis- and tris-prolinamide derivatives used in this study. Since proline residues are present in numerous bioactive peptides, this class of molecules may exhibit biological activities. Ligand **Pro-4** shows cytotoxicity towards HepG2 cells and it is able to down-regulate *c-MYC* expression in cancer cells. AFM studies indicate that **Pro-4** can direct the formation of *c-MYC* G-quadruplex higher order nanostructures, which may be useful for the development of novel devices, with medical and nanotechnology applications.

Experimental section

FRET melting experiments

Stock solutions of 2 μM concentration of each prolinamide compounds (**Pro-1**, **Pro-2**, **Pro-3** and **Pro-4**) were prepared in MQ water. Four dual fluorescently labeled DNA oligonucleotide sequences were diluted in 50 mM potassium cacodylate buffer, pH 7.4.

c-MYC: 5′-*FAM*-d($TGAG_3TG_3TAG_3TG_3TA_2$)-*TAMRA*-3′

h-TELO: 5′-($G_3TTAG_3TTAG_3TTAG_3$)-3′

c-KIT1: 5′-*FAM*-d($G_3AG_3CGCTG_3AG_3AG_3$)-*TAMRA*-3′,

c-KIT2: 5′-*FAM*-d($G_3CG_3CGCGAG_3AG_4$)-*TAMRA*-3′

and

ds DNA: 5′-*FAM*-d(CCAGTTCGTAGTAACCC)-3′/3′-*TAMRA* (GGTCAAGCATCATTGGG)-5′

The donor fluorophore was 6-carboxyfluorescein, FAM, and the acceptor fluorophore was 6-carboxytetramethylrhodamine, TAMRA. The dual-labeled DNA was annealed at a concentration of 400 nM by heating at 95 °C for 5 min followed by cooling to room temperature. The 96-well plates were prepared by aliquoting 50 μL of the annealed DNA into each well, followed by 50 μL of the carbazole compounds. For competition experiments, duplex competitors were added to 200 nM quadruplex sequences at final concentrations of 3.0 μM and 10.0 μM. The concentration of **Pro-4** is kept at 1.0 μM. For FRET titration experiments, different concentrations of **Pro 3** and **Pro 4** were added to 200 nM of all four DNA sequences. Measurements were made in triplicate with an excitation wavelength of 483 nm and a detection wavelength of 533 nm using a LightCycler® 480-II System RT-PCR machine (Roche). Final analysis of the data was carried out using Origin Pro 8 data analysis.

Fluorescence binding experiments

Fluorescence quenching measurements were performed using a fluorescence spectrophotometer (Fluorolog-3-Horiba). Stock solution of 500 nM of 5′-FAM or 3′-FAM labeled *c-MYC* in a 10 mM Tris-HCl, pH 7.5, and 100 mM KCl buffer was prepared. 500 μM stock solutions of ligands **Pro-3** and **Pro-4** were prepared. The ligands were added to the labeled *c-MYC* in a stepwise manner and the fluorescence spectrum was recorded. Fluorescence excitation was set at 480 nm and emission was monitored at 522 nm. Bandwidths of both excitation and emission filters were set at 4 nm. Fluorescence quenching was observed after the incremental addition of **Pro-3** or **Pro-4**. The value of binding constant was determined by using eqn (S4) (see the ESI† for details).

TO displacement assay

0.25 μM of pre-folded quadruplexes and duplex were mixed with thiazole orange (0.50 μM TO) in buffer containing 100 mM KCl and 10 mM Tris·HCl, pH 7.4. Ligands **Pro 3** and **Pro 4** were added to the mixture stepwise in the same buffer with a 3 min equilibration period and the fluorescence spectrum was recorded. The percentage of displacement was

calculated from the fluorescence area (FA, 510–700 nm, λ_{ex} = 501 nm), using,

$$\text{TO displacement}(\%) = 100 - [\text{FA} \times 100/\text{FA}_0] \quad (1)$$

FA_0 being the fluorescence area from TO bound to the DNA without added ligands. The percentages of displacements were then plotted as a function of the concentration of the ligands.

qRT-PCR analysis

To evaluate the role of tris-prolinamide derivatives at the transcriptional level of *c-MYC*, qRT-PCR was performed. Cancer cells were incubated with an IC_{50} dose (13.4 μM and 7.1 μM) of **Pro-3** and **Pro-4** for 24 h at 37 °C in a humidified 5% CO_2 incubator. Total RNA was prepared from compound treated and untreated HepG2 cells using the trizol kit according to the manufacturer's protocol (Invitrogen Corporation). A cDNA library was prepared by using the High Capacity cDNA Reverse Transcription Kit (Applied Biosystems). Master mix (2×) was prepared from 2 μL 10× RT buffer, 0.8 μL 25× 100 mM dNTP mix, 2 μL 10× RT random primer, 1 μL of reverse transcriptase, 1 μL of RNase inhibitor and 3.2 μL nuclease free water. 10 μL 2× master mix was added to a 10 μL sample and sealed in 96 well plates. Reverse transcription reaction was performed on a Light Cycler 480 II (Roche). The thermal cycling condition was programmed as 10 min at 25 °C, 120 min at 37 °C and 5 min at 85 °C for one single cycle. Real-time RT-PCR was performed on a Light Cycler 480 II (Roche) with the SYBR green JumpStart TaqReadyMix (Sigma, Saint Louis, USA) reagent using the cDNA library as the template. The primers used for the real-time RT-PCR analyses had the following sequences:[28,29]

c-MYC (forward): 5′-CTGCGACGAGGAGGAGGACT-3′
c-MYC (reverse): 5′-GGCAGCAGCTCGAATTTCTT-3′
GAPDH (forward): 5′-GACGGCCGCATCTTCTTGT-3′
GAPDH (reverse): 5′-CACACCGACCTTCACCATTTT-3′

The PCR mixture (25 μL) contained 15 pmol of each primer, 7 μL of water, 5 μL of cDNA, and 12.5 μL 2× JumpStart Taq ReadyMix. The samples were placed in 96-well plates (Roche), and PCR amplification was performed using the Light Cycler 480 II real-time PCR detection system (Roche). The thermal cycling conditions were 2 min at 94 °C and then 40 cycles of 15 s at 94 °C, followed by 60 s at 60 °C. We used the comparative cycle threshold method (C_T method) for the relative quantification of gene expression.[30] The C_T for the target and the C_T for the internal control (GAPDH) were determined for **Pro-3** and **Pro-4** or untreated (control) samples. Finally, the arithmetic calibrator ($2^{-\Delta\Delta C_T}$) was used to calculate the relative mRNA level expression of *c-MYC*. Difference in *c-MYC* expression was expressed as fold changes.

Western blot analysis

Liver carcinoma HepG2 cells were treated with an IC_{50} dose (13.4 μM and 7.1 μM) of **Pro-3** and **Pro-4** for 24 h at 37 °C in a humidified CO_2 incubator. After the incubation period, the cells were washed once with PBS (pH 7.4) and then lysed with cold cell lysis buffer (20 mM Tris, 100 mM NaCl, 1 mM EDTA in 0.5% Triton X-100). The lysed cells were collected from the treated and untreated cells, and the total protein content was estimated by the Lowry method.[31] Equal amounts of proteins (60 μg) from the lysed cells were separated by 10% SDS-PAGE and transferred to nitrocellulose membranes. The membranes were blocked, washed and probed using antibodies directed against *c-MYC* and GAPDH (as loading control) overnight at room temperature. The blots were washed and immunoreactive bands were incubated with a 1 : 2000 dilution of the ALKP conjugated secondary antibody for 2 h at room temperature. Binding signals were visualized with the NBD/BCIP substrate. Relative band intensities were determined by using ImageJ software.

Acknowledgements

This work was supported by the Council of Science and Industrial Research (CSIR) and the Department of Biotechnology (DBT) India. SP thanks CSIR for a research fellowship and MD thanks the Department of Science and Technology (DST) for an INSPIRE research fellowship.

References

1 M. Gellert, M. N. Lipsett and D. R. Davies, *Proc. Natl. Acad. Sci. U. S. A.*, 1962, **48**, 2013.
2 (*a*) D. Sen and W. Gilbert, *Nature*, 1988, **334**, 364; (*b*) V. S. Chambers, G. Marsico, J. M. Boutell, M. Di Antonio, G. P. Smith and S. Balasubramanian, *Nat. Biotechnol.*, 2015, **33**, 877.
3 T. A. Brooks and L. H. Hurley, *Nat. Rev. Cancer*, 2009, **9**, 849.
4 V. González and L. H. Hurley, *Annu. Rev. Pharmacol. Toxicol.*, 2010, **50**, 111.
5 (*a*) S. Balasubramanian and S. Neidle, *Curr. Opin. Chem. Biol.*, 2009, **13**, 345; (*b*) S. Balasubramanian, L. H. Hurley and S. Neidle, *Nat. Rev. Drug Discovery*, 2011, **10**, 261.
6 A. Siddiqui-Jain, C. L. Grand, D. J. Bearss and L. H. Hurley, *Proc. Natl. Acad. Sci. U. S. A.*, 2002, **99**, 11593.
7 G. W. Collie and G. N. Parkinson, *Chem. Soc. Rev.*, 2011, **40**, 5867.
8 (*a*) J. Seenisamy, S. Bashyam, V. Gokhale, H. Vankayalapati, D. Sun, A. Siddiqui-Jain, N. Streiner, K. Shin-ya, E. White, W. D. Wilson and L. H. Hurley, *J. Am. Chem. Soc.*, 2005, **127**, 2944–2959; (*b*) Y. P. Kumar, S. Bhowmik, R. N. Das, I. Bessi, S. Paladhi, R. Ghosh, H. Schwalbe and J. Dash, *Chem. – Eur. J.*, 2013, **19**, 11458; (*c*) H. R. Nasiri, N. M. Bell, K. I. E. McLuckie, J. Husby, C. Abell, S. Neidle and S. Balasubramanian, *Chem. Commun.*, 2014, **50**, 1704; (*d*) M. Zuffo, F. Doria, V. Spalluto, S. Ladame and M. Freccero, *Chem. – Eur. J.*, 2015, **21**, 17596; (*e*) F. Doria, A. Oppi, F. Manoli, S. Botti, N. Kandoth, V. Grande, I. Manet and M. Freccero, *Chem. Commun.*, 2015, **51**, 9105.

9 E. Izbicka, R. T. Wheelhouse, E. Raymond, K. K. Davidson, R. A. Lawrence, D. Sun, B. E. Windle, L. H. Hurley and D. D. Von Hoff, *Cancer Res.*, 1999, **59**, 639.

10 (*a*) T.-M. Ou, Y.-J. Lu, C. Zhang, Z.-S. Huang, X.-D. Wang, J.-H. Tan, Y. Chen, D.-L. Ma, K.-Y. Wong, J. C.-O. Tang, A. S.-C. Chan and L.-Q. Gu, *J. Med. Chem.*, 2007, **50**, 1465; (*b*) J. Dai, M. Carver, L. H. Hurley and D. Yang, *J. Am. Chem. Soc.*, 2011, **133**, 17673; (*c*) T.-M. Ou, J. Lin, Y.-J. Lu, J.-Q. Hou, J.-H. Tan, S.-H. Chen, Z. Li, Y.-P. Li, D. Li, L.-Q. Gu and Z.-S. Huang, *J. Med. Chem.*, 2011, **54**, 5671.

11 J. Dash, P. S. Shirude and S. Balasubramanian, *Chem. Commun.*, 2008, 3055.

12 (*a*) P. V. L. Boddupally, S. Hahn, C. Beman, B. De, T. A. Brooks, V. Gokhale and L. H. Hurley, *J. Med. Chem.*, 2012, **55**, 6076; (*b*) D. Panda, M. Debnath, S. Mandal, I. Bessi, H. Schwalbe and J. Dash, *Sci. Rep.*, 2015, **5**, 13183; (*c*) K. M. Felsenstein, L. B. Saunders, J. K. Simmons, E. Leon, D. R. Calabrese, S. Zhang, A. Michalowski, P. Gareiss, B. A. Mock and J. S. Schneekloth Jr., *ACS Chem. Biol.*, 2016, **11**, 139.

13 (*a*) J. T. Davis, *Angew. Chem., Int. Ed.*, 2004, **43**, 668; (*b*) P. Alberti, A. Bourdoncle, B. Sacca, L. Lacroix and J.-L. Mergny, *Org. Biomol. Chem.*, 2006, **4**, 3383; (*c*) K. J. Neaves, J. L. Huppert, R. M. Henderson and J. M. Edwardson, *Nucleic Acids Res.*, 2009, **37**, 6269; (*d*) I. Mela, R. Kranaster, R. M. Henderson, S. Balasubramanian and J. M. Edwardson, *Biochemistry*, 2012, **51**, 578; (*e*) N. Zhang, X. Chu, M. Fathalla and J. Jayawickramarajah, *Langmuir*, 2013, **29**, 10796; (*f*) A. D. R. Pontinha, A.-M. Chiorcea-Paquim, R. Eritja and A. M. Oliveira-Brett, *Anal. Chem.*, 2014, **86**, 5851; (*g*) R. N. Das, M. Debnath, A. Gaurav and J. Dash, *Chem. – Eur. J.*, 2014, **20**, 16688.

14 A. Chauhan, S. Paladhi, M. Debnath, S. Mandal, R. N. Das, S. Bhowmik and J. Dash, *Bioorg. Med. Chem.*, 2014, **22**, 4422.

15 J. E. Moses, D. J. Ritson, F. Zhang, C. M. Lombardo, S. Haider, N. Oldham and S. Neidle, *Org. Biomol. Chem.*, 2010, **8**, 2926.

16 S. Paladhi, J. Das, P. K. Mishra and J. Dash, *Adv. Synth. Catal.*, 2013, **355**, 274.

17 (*a*) R. A. J. Darby, M. Sollogoub, C. McKeen, L. Brown, A. Risitano, N. Brown, C. Barton, T. Brown and K. R. Fox, *Nucleic Acids Res.*, 2002, **30**, e39; (*b*) R. J. Harrison, A. P. Reszka, S. M. Haider, B. Romagnoli, J. Morrell, M. A. Read, S. M. Gowan, C. M. Incles, L. R. Kelland and S. Neidle, *Bioorg. Med. Chem.*, 2004, **14**, 5845; (*c*) A. De Cian, L. Guittat, M. Kaiser, B. Saccà, S. Amrane, A. Bourdoncle, P. Alberti, M.-P. Teulade-Fichou, L. Lacroix and J.-L. Mergny, *Methods*, 2007, **42**, 183.

18 (*a*) J. Alzeer, B. R. Vummidi, P. J. C. Roth and N. W. Luedtke, *Angew. Chem., Int. Ed.*, 2009, **48**, 9362; (*b*) J. Alzeer and N. W. Luedtke, *Biochemistry*, 2010, **49**, 4339; (*c*) D. D. Le, M. Di Antonio, L. K. M. Chan and S. Balasubramanian, *Chem. Commun.*, 2015, **51**, 8048.

19 S. Ghosh, C. Ghosh, S. Nandi and K. Bhattacharyya, *Phys. Chem. Chem. Phys.*, 2015, **17**, 8017.

20 (*a*) D. Monchaud, C. Allain and M.-P. Teulade-Fichou, *Bioorg. Med. Chem.*, 2006, **16**, 4842; (*b*) P. L. T. Tran, E. Largy, F. Hamon, M.-P. Teulade-Fichou and J.-L. Mergny, *Biochimie*, 2011, **93**, 1288.

21 (*a*) Y. Xu, T. Ishizuka, K. Kurabayashi and M. Komiyama, *Angew. Chem., Int. Ed.*, 2009, **48**, 7833; (*b*) A. Rajendran, M. Endo, K. Hidaka and H. Sugiyama, *Angew. Chem., Int. Ed.*, 2014, **53**, 4107.

22 (*a*) A. Rajendran, M. Endo, K. Hidaka, P. L. Thao Tran, M.-P. Teulade-Fichou, J.-L. Mergny and H. Sugiyama, *RSC Adv.*, 2014, **4**, 6346; (*b*) A. Laguerre, Y. Chang, M. Pirrotta, N. Desbois, C. P. Gros, E. Lesniewska and D. Monchaud, *Org. Biomol. Chem.*, 2015, **13**, 7034.

23 (*a*) L. Petraccone, J. O. Trent and J. B. Chaires, *J. Am. Chem. Soc.*, 2008, **130**, 16530; (*b*) S. Haider, G. N. Parkinson and S. Neidle, *Biophys. J.*, 2008, **95**, 296; (*c*) S. M. Haider and S. Neidle, *Biochem. Soc. Trans.*, 2009, **37**, 583; (*d*) L. Petraccone, N. C. Garbett, J. B. Chaires and J. O. Trent, *Biopolymers*, 2010, **93**, 533.

24 (*a*) P. Hazel, G. N. Parkinson and S. Neidle, *J. Am. Chem. Soc.*, 2006, **128**, 5480; (*b*) K.-i. Shinohara, Y. Sannohe, S. Kaieda, K.-i. Tanaka, H. Osuga, H. Tahara, Y. Xu, T. Kawase, T. Bando and H. Sugiyama, *J. Am. Chem. Soc.*, 2010, **132**, 3778; (*c*) L. Stefan, F. Denat and D. Monchaud, *J. Am. Chem. Soc.*, 2011, **133**, 20405.

25 A. Ambrus, D. Chen, J. Dai, R. A. Jones and D. Yang, *Biochemistry*, 2005, **44**, 2048.

26 (*a*) D. Monchaud and M.-P. Teulade-Fichou, *Org. Biomol. Chem.*, 2008, **6**, 627; (*b*) S. A. Ohnmacht and S. Neidle, *Bioorg. Med. Chem. Lett.*, 2014, **24**, 2602.

27 T. Mosmann, *J. Immunol. Methods*, 1983, **65**, 55.

28 C.-H. Wu, J. van Riggelen, A. Yetil, A. C. Fan, P. Bachireddy and D. W. Felsher, *Proc. Natl. Acad. Sci. U. S. A.*, 2007, **104**, 13028.

29 P. Velica, N. J. Davies, P. P. Rocha, H. Schrewe, J. P. Ride and C. M. Bunce, *Mol. Cancer*, 2009, **8**, 121.

30 F. Leite, S. O'Brien, M. J. Sylte, T. Page, D. Atapattu and C. J. Czuprynski, *Infect. Immun.*, 2002, **70**, 4336.

31 O. H. Lowry, N. J. Rosebrough, A. L. Farr and R. J. Randall, *J. Biol. Chem.*, 1951, **193**, 265.